

Investigation on All-Optical Clock Recovery from RZ-Format Data at 64Gbit/s by Using a Two-Section Index-Coupled DFB Laser *

Wu Tong, Qiu Kun

Key Lab of Broadband Optical Fiber Transmission and Communication Networks, UEST of China, Chengdu 610054

Abstract High speed all-optical clock recovery from 64Gbit/s RZ-format PRBS data by using a two-section index-coupled distributed feedback (DFB) laser is simulated and demonstrated. The performance of it such as timing jitter, lockup time, locking range are described and analyzed in detail.

Keywords Optical clock recovery; Self pulsation; Distributed feedback (DFB) laser; Injection locking

CLCN TN913.24 Document Code A

0 Introduction

Future optical networks are expected to employ not only optical transmission but also some level of optical signal processing. Because an optical clock is needed for triggering the signal processing functions, the all-optical clock recovery circuit is a critical component in high speed digital optical communication systems.

All-optical clock recovery has been demonstrated using actively mode-locked fiber lasers^[1], passively mode-locked semiconductor lasers^[2], self-pulsation in multi-section gain-coupled^[3,4]/index-coupled^[5] DFB laser diodes. Of the various techniques, DFB lasers are of significant interest because they have such advantages as compactness, high speed, and wide-locking range.

The clock recovery using DFB lasers is based on self-pulsation and injection locking in DFB lasers. In this paper, the capability of a two-section index-coupled DFB in all-optical clock recovery by using numerical simulation and describe the performance will be studied in detail.

1 Setups of the simulation system

The clock recovery is simulated using a commercial software by Virtual Photonics. In this simulation platform, the laser is modeled based on

the transmission-line laser model (TLLM), which is a dynamic, multimode, time-domain model that is able to simulate the dynamic and static spectra and power characteristics of many types of laser.

The DFB laser comprises an optical grating along the optical waveguide which provides a strong optical feedback into the center of the cavity at certain wavelengths. The TLLM is easily modified to include such feedback by adding impedance mismatches along the model. An easy way to think of the model is alternate low- and high-impedance transmission-line sections^[6].

At the boundaries between the lines there will be coupling between the forward and backward waves due to the impedance mismatches, which can be represented by a simple modification to the connection matrix and the scattering matrix. This coupling is direct analog to that in the DFB laser, and so accurate simulation is possible^[6].

The simulation system consists of a TS-DFB clock recovery module, a PRBS generator and a transmission module.

The TS-DFB simulation module is composed by two identical index-coupled DFB laser with uniform grating. Each section is with a length of 400 μm , and biased at, respectively, 56 mA and 87.5 mA. Their $|\kappa L|$ equal to 2 both. Table. 1 gives other parameter and its' value used in simulation.

Table. 1 Values of the parameters used in simulation

Material differential gain	3.0e-20	m^2	Material linewidth enhancement factor	4.86
Confinement factor	0.35		Transparency carrier density	1.5e+24 $1/\text{m}^3$
Initial carrier density	2.14e+24	$1/\text{m}^3$	Thickness of the active layer	0.18e-6 m
Width of the active layer	3.5e-6	m	Auger recombination coefficient	3e-41 m^6/s
Group effective index	3.7		Bimolecular recombination coefficient	1e-16 m^3/s

The 64 Gbit/s RZ PRBS signal is generated by

following steps; the 16 Gbit/s RZ PRBS electronic signal is modulated onto optical pulses at a 16 GHz repetition rate via a MZI modulator; this optical signal is then injected into a two-stage optical time-

* Supported by TRAPOYT

Tel: 028-83200274 Email: pegasusme@163.com

Received date: 2004-06-21

division multiplexer to generate the 64 Gbit/s RZ PRBS optical signal. In multiplexer, we set τ_1 equal to 31 ps and τ_2 equal to 16ps to simulate the timing jitter produced by a real time-division multiplexer.

This PRBS signal will be launched into a transmission module before being injected into TS-DFB module, shown as Fig. 1. The SMF have a

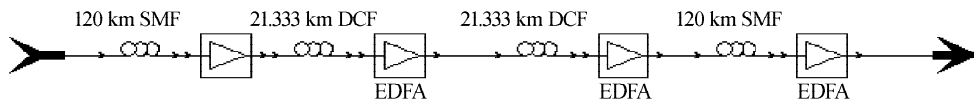


Fig. 1 Fabric of the transmission module

2 Simulation testing and analysis

2.1 Self-Pulsation

Fig. 2, Fig. 3 show the optical spectrum and the RF spectrum of the laser's output in free-running state respectively. We can get a sight of two laser mode in Fig. 2. Their frequency detuning is 65.625 GHz, and equals to the self-pulsation frequency measured from Fig. 3, which confirms the mechanism of beating type self-pulsation^[7].

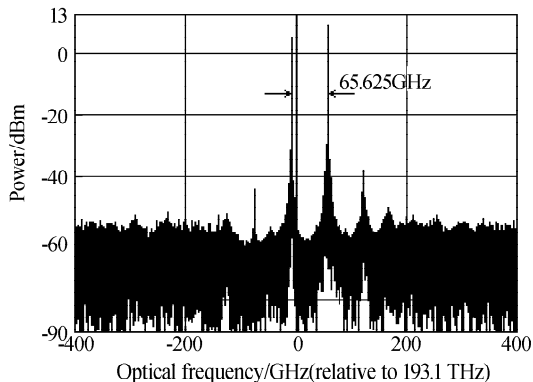


Fig. 2 Optical spectrum of the free-running state

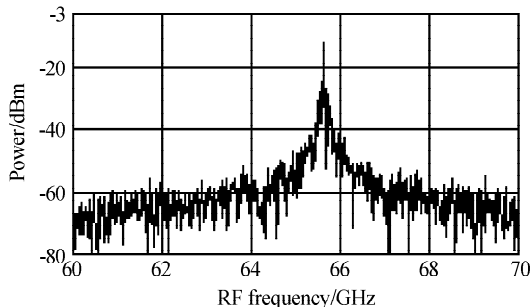


Fig. 3 RF spectrum of the free-running state

The frequency of self-pulsation can be controlled by changing the dc bias of each DFB section. We get the SP frequency of 30 GHz~75 GHz by adjusting I_1 while fixing I_2 at 87.5 mA.

2.2 Injection locking & clock recovery

We set the RZ PRBS signal at 1553.15 nm, which corresponds to the second laser mode of the DFB. In this situation, the DFB will work on the coherent injection locking mode^[3]. The average power of signal after the transmission module measures -6.26 dBm. Fig. 4, Fig. 5 show the

attenuation of 0.2×10^{-3} dB/m, a dispersion of 160.0×10^{-6} s/m², a dispersion slope of 0.08 s/m³ and a nonlinear index of 2.6×10^{-20} m²/W. The DCF have a attenuation of 0.6×10^{-3} dB/m, a dispersion of -90.0×10^{-6} s/m², a dispersion slope of 0.21 s/m³ and a nonlinear index of 4.0×10^{-20} m²/W.

RF spectrum and power waveform of the laser's output in locking state.

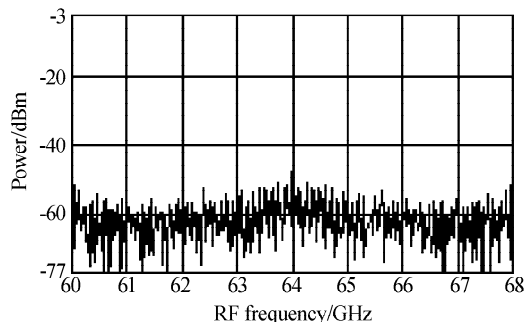


Fig. 4 RF spectrum of the recovered clock

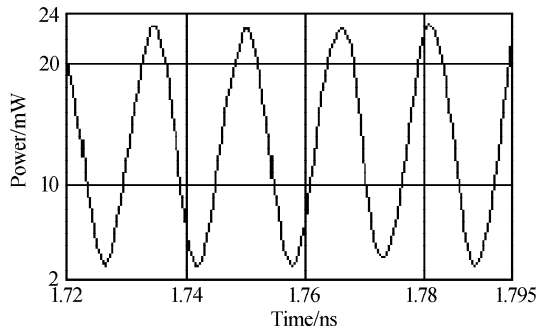


Fig. 5 Power waveform of the recovered clock

By comparing Fig. 3 and Fig. 4 one can see the injection locking clearly: the self-pulsation peak shifts from 65.525 GHz to 64 GHz which is the clock frequency of the injection signal. Meanwhile, the linewidth (FWHM) of the RF signal becomes very narrow.

The recovered clock signal we get at the output of the laser has a pulse width (FWHM) of averaged 8.75 ps, a carrier-to-noise ratio of 37 dB with 8.6 dB extinction ratio.

2.3 Locking range

If the frequency detuning of the self-pulsation frequency in free-running state and the clock frequency of signal is too large, injection locking cannot take place. The locking range $\Delta\Omega_L$ is the maximum detuning permitted for clock recovery, given by^[7]

$$\Delta\Omega_L = (\Omega_{in} - \Omega_0)_{max} = \kappa \frac{|P_{in}|}{|\bar{P}_1^{lock}|} \quad (1)$$

where $|\bar{P}_1^{lock}|$ is the average output power of laser

in locked state, $|P_{in}|$ is the average injected power. From Eq. 4, a direct proportion between the locking range and the injected power can be found.

The locking range under different injection power is investigated and plotted in Fig. 6, in which circles represent the simulation results and the line the fitted curve, the central frequency is 65.625 GHz which is the self-pulsation frequency in the free-running state. A linear relation, which corresponds to Eq. 4, is observed from Fig. 6 and we can see the larger the injected power, the wider the locking range. But we also find that the output pulses are distorted when the injected power is too strong (about 3 mW in this simulation module). It is because of the strong modulation effect in carrier density caused by strong injection power.

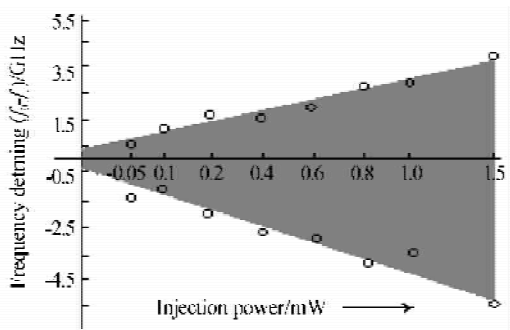


Fig. 6 Locking range as a function of the injected power

2.4 Lockup time

Lockup time is defined as the time interval between the application of the injection signal and the synchronization of the laser. And the system latency will be affected by this parameter.

To investigating the lockup time, the PRBS generator is modified to generate a short series of “1”s (50 bits) followed by a long series of “0”s (500 bits) alternately. By analyzing the waveform of the output pulses, we find that the output pulses will stably synchronize to the clock signal of the input data after about 12 b, which is 187.5 ps, with -6.26 dBm injection power.

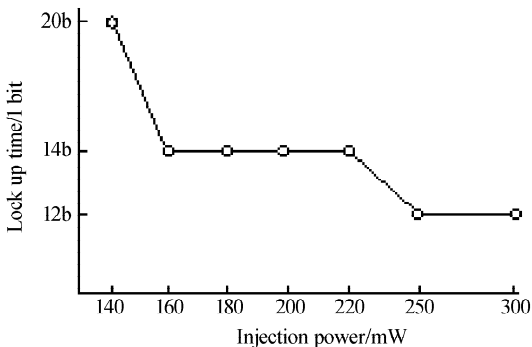


Fig. 7 The relationship between lockup time and the injection power

We also investigate the relationship between the lockup time and the injection power by

changing the power of the injection signal. We find that the time needed to lockup decreases with an increase of the injected power (Fig. 7), but it will keep a constant when the power of the injected signal reaches a threshold.

2.5 Timing jitter

By investigating the timing jitter of the transmitted signal and the recovered clock, we can evaluate the stability of the clock recovery system.

From the eye diagram (Fig. 8 and Fig. 9), we estimate that the timing jitter of the transmitted signal (σ_{ct}) is 4ps and the timing jitter of the recovered clock (σ_{cc}) is less than 1 ps.

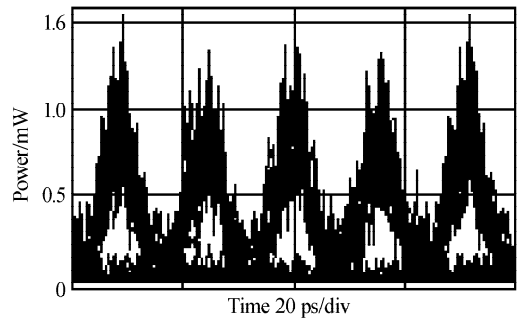


Fig. 8 Eye diagram of the transmitted PRBS signal

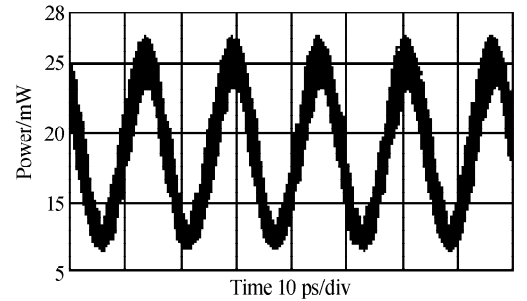


Fig. 9 Eye diagram of the recovered clock pulses

Because the timing jitter measurements directly from the eye diagram are not always reliable, we also calculate the timing jitter from phase-noise measurement. The RMS timing jitter can expressed by^[8]

$$\sigma_c = \frac{1}{2\pi n f} \sqrt{\frac{p_n}{p_c} \frac{\Delta f}{RB}} \quad (2)$$

where n is the harmonic number (here, $n=1$), and RB is the resolution bandwidth of the RF spectrum analyzer, and p_n and p_c are the power of the n th harmonics and the maximum of the phase noise centered on the harmonics, and Δf is the noise bandwidth (FWHM), and f is the clock frequency.

These parameters, shown in Table. 2, are measured at the RF spectrum.

Table. 2 Parameters for computing RMS timing Jitter

	p_c/p_n	RB	Δf
Transmitted signal	26 dB	100 kHz	74.4 MHz
Recovered clock	38 dB	50 kHz	11.55 MHz

The computed timing jitter are: $\sigma_{ct} = 3.4$ ps

and $\sigma_{cc}=0.475$ ps respectively, a little smaller than that measured from eye diagram.

2.6 Pattern effect

Finally, the pattern effect in this clock recovery module is studied by inject four different length of PRBS signals namely 2^7-1 , $2^{15}-1$, $2^{23}-1$, $2^{31}-1$ into the DFB laser, which average power are -6.26dBm. The timing jitter, CNR, extinction ratio and power waveform of the output clock pulses of each situation are tested and compared, and we find that they coincide with each other well i. e. the clock recovery module consists of the two-section index-coupled DFB laser has few pattern effect.

3 Conclusion

A two-section index-coupled DFB laser emulational model is fabricated and its capability for all-optical clock recovery from 64Gbit/s RZ-format PRBS signal is investigated by using numerical simulation. The performance such as timing jitter, lockup time, locking range are analyzed in detail. By optimizing parameters of the laser, the recovered clock pulses have a RMS timing jitter of 0.475 ps ($\sim 3\%$), a extinction ratio of 8.6 dB and a carrier-to-noise ratio of 38 dBm with -6.26 dBm injection power, which demonstrated the high quality of this clock recovery module. Values of parameters obtained in simulation are useful for further practical

investigation.

References

- 1 Bigo S, Leclerc O, Desurvire E. All-optical fiber signal processing and regeneration for soliton communications. *IEEE Journal of Selected Topics in Quantum Electronics*, 1997, **3**(6): 1208~1223
- 2 Ludwig R, Ehrhardt A, Pieper W, et al. 40 Gbit/s demultiplexing experiment with 10 GHz all-optical clock recovery using a modelocked semiconductor laser. *Electronics Letters*, 1996, **32**(4): 327~329
- 3 Mao W, Li Y, Al-Mumin M, et al. 40 Gbit/s all-optical clock recovery using two-section gain-coupled DFB laser and semiconductor optical amplifier. *Electronics Letters*, 2001, **37**(21): 2030~2039
- 4 Mao W, Li Y, Al-Munin M, et al. All-optical clock recovery from RZ-format data by using a two-section gain-coupled DFB laser. *IEEE Journal of Lightwave Technology*, 2002, **28**(9): 8~10
- 5 Sartorius B, Mohrle M, Feiste U. 12 to 64 GHz continuous frequency tuning in self-pulsating 1.55 μm multiquantum-well DFB lasers. *IEEE Journal of Selected Topics in Quantum Electronics*, 1995, **1**(2): 535~538
- 6 Virtual Photonics Inc. Active Photonics User's Manual. VPI, 2000. 5-11~5-12
- 7 Duan G H, Pham G. Injection-locking properties of self pulsation in semiconductor lasers. *IEEE Photonics Technology Letters*, 1997, **14**(4): 228~231
- 8 Wang T, Lou C Y, Huo L, et al. Combination of comb-like filter and SOA for preprocessing to reduce the pattern effect in the clock recovery. *IEEE Photonics Technology Letters*, 2004, **16**(2): 613~614

基于双区折射率耦合 DFB 激光器实现 64 Gbit/s 归零编码数据全光时钟恢复研究

武同邱昆

(电子科技大学宽带光纤传输与通信网技术重点实验室, 成都 610054)

收稿日期: 2004-06-21

摘要 使用双区折射率耦合 DFB 激光器对 64 Gbit/s 归零伪随机二进制序列 (PRBS) 信号的时钟恢复进行了仿真实验, 并通过实验结果仔细分析了信号时间抖动, 激光器锁定时间, 锁定范围等评估时钟恢复系统性能的参数。

关键词 光时钟恢复; 自脉动; 分布反馈激光器; 注入锁定



Wu Tong was born in 1980. He received the B. S. degree from University of Electronic Science and Technology of China, in 2002. Currently he is pursuing his M. S. degree at the Key Lab of Broadband Optical Fiber Transmission and Communication Networks, UEST of China, Chengdu. His research activities are in key technologies of optical packet switching and all optical signal processing.